

# GEM Detectors for COMPASS

B. Ketzer, S. Bachmann, M. Capeáns, M. Deutel, J. Friedrich, S. Kappler, I. Konorov, S. Paul, A. Placci, K. Reisinger, L. Ropelewski, L. Shekhtman, and F. Sauli

**Abstract**—For the small-area tracking of particles within COMPASS (common muon and proton apparatus for structure and spectroscopy), a new fixed target experiment at CERN/SPS, several large-size ( $31 \times 31 \text{ cm}^2$ ) detectors based on the gas electron multiplier (GEM), have been built. These new devices, consisting of several GEM amplification stages with a two-coordinate readout, combine good spatial resolution with high rate capability, which is required by the large particle flux near the beam. At the same time, the material exposed to the beam is minimized in order not to spoil the mass resolution of the spectrometer. The first detectors out of a total of 20 were subject to extensive tests in the beam and in the laboratory, showing that full (i.e.,  $>98\%$ ) detection efficiency for minimum ionizing particles can be achieved at a total effective gain of 6000. Ongoing research work focuses on discharges triggered by heavily ionizing particles entering the detectors. Systematic studies of the energy released in discharges and their probability of occurring at all as a function of a variety of parameters suggest several means to minimize their impact on detector performance. First results of the operational characteristics of these detectors in the real COMPASS beam are presented.

**Index Terms**—Gas detectors, gas electron multiplier, high-rate tracking, position-sensitive particle detectors, radiation detectors, spectroscopy.

## I. INTRODUCTION

THE GOAL of COMPASS (common muon and proton apparatus for structure and spectroscopy), a new fixed target experiment currently under construction at CERN's Super Proton Synchrotron (SPS), is the investigation of hadron structure and hadron spectroscopy using muon and hadron beams at intensities of up to  $2 \cdot 10^8$  particles ( $\mu$ -beam) and  $1 \cdot 10^8$  particles (hadron beam) per SPS spill of 2.2 s, respectively [1]. One of the main topics to be addressed in the first runs is the measurement of the gluon polarization  $\Delta G/G$ , both from the cross-section asymmetry for open charm production in deep inelastic scattering of polarized muons on polarized nucleons and from asymmetries in the production of high- $p_T$  hadron jets. Using hadron beams, we will study the hadronic structure of unstable particles using virtual photons (Primakoff scattering), as well as charmed hadrons and exotic hadrons like glueballs and hybrids.

Fig. 1 shows the experimental setup of COMPASS, which comprises a two-stage magnetic spectrometer, with each of the

stages being equipped with small- and large-area tracking, a fast RICH detector for particle identification, electromagnetic and hadronic calorimetry, and muon identification.

For the large-area tracking throughout both stages of the spectrometer, wire chambers of various designs will be used. The small-area tracking of particles near the beam, where high location accuracy over a relatively large area is required and the particle flux is large, will be achieved by micropattern gas detectors. In the muon beam, Micromegas [2], optimized to obtain a time resolution better than 10 ns, will be used before the first spectrometer magnet (SM1 in Fig. 1), where the background of particles coming from the target has not yet been swept away by the magnetic field. Downstream of SM1, 20 multistep GEM detectors [3] will form ten tracking stations, each comprising two GEM detectors, one being rotated by  $45^\circ$  with respect to the other. These detectors are being built using as little material as possible in order not to spoil the mass resolution of the spectrometer, with one detector only accounting for about  $5 \lambda_{\text{rad}}$  of radiation length. In addition, the use of several cascaded GEM amplification stages makes this particular type of detector less susceptible to discharges under exposure to heavily ionizing particles and permits the GEM detectors to be used also in the hadron beam of COMPASS.

## II. THE GEM DETECTORS

The GEM ([4] and references therein) is made from a thin Cu-clad Kapton foil,  $50\text{-}\mu\text{m}$  thick with Cu layers of  $5 \mu\text{m}$ , which has been chemically perforated by a large number of holes of  $\sim 70 \mu\text{m}$  diameter, separated by a distance of  $\sim 140 \mu\text{m}$ . Added between a drift electrode and the readout strips of a gaseous detector, the (normally parallel) field lines are compressed into the holes when a potential difference  $\Delta U_{\text{GEM}}$  is applied between the two Cu layers of the foil. At  $\Delta U_{\text{GEM}} \approx 550 \text{ V}$ , gas amplification factors of several thousand have been achieved in a single foil, without additional amplification in the gaps between drift and GEM foil and GEM and readout plane, respectively, the electric fields there being  $E \sim 3\text{--}4 \text{ kV/cm}$ . As a consequence, the readout strips in such a purely GEM-based detector can remain on ground potential. The signal on the strips is entirely due to electron collection and therefore intrinsically fast, since the GEM foil efficiently shields the tail due to the slow motion of ions usually present in gaseous devices.

Since there is little loss of charge in the foil, several GEM amplification stages can be cascaded in a detector in order to achieve gains of several tens of thousand, while still operating each foil at moderate voltages. For COMPASS, the first prototypes consist of two multiplication stages, separated by a gap of 2 mm. The distance of the first GEM foil to the drift electrode is 3 mm, while the induction gap to the readout is 2 mm, as shown in Fig. 2. The de-

Manuscript received October 30, 2000.

B. Ketzer, S. Bachmann, M. Deutel, A. Placci, K. Reisinger, L. Ropelewski, and F. Sauli are with CERN, the European Laboratory for Particle Physics, Geneva 23, Switzerland (e-mail: Bernhard.Ketzer@cern.ch).

M. Capeáns is with Universität Heidelberg, Heidelberg 69117, Germany.

J. Friedrich, I. Konorov, and S. Paul are with Technische Universität München, Garching 85748, Germany.

S. Kappler is with Universität Karlsruhe, Karlsruhe 76128, Germany.

L. Shekhtman is with CERN, the European Laboratory for Particle Physics, Geneva 23, Switzerland, and the Budker Institute of Nuclear Physics, Novosibirsk 630090, Russia.

Publisher Item Identifier S 0018-9499(01)07025-3.

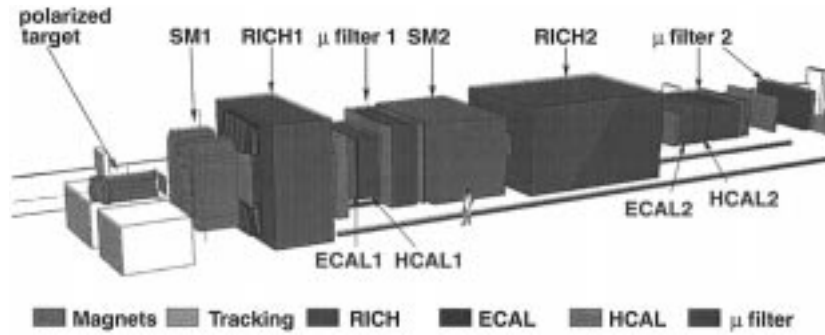


Fig. 1. Experimental setup of the COMPASS spectrometer.

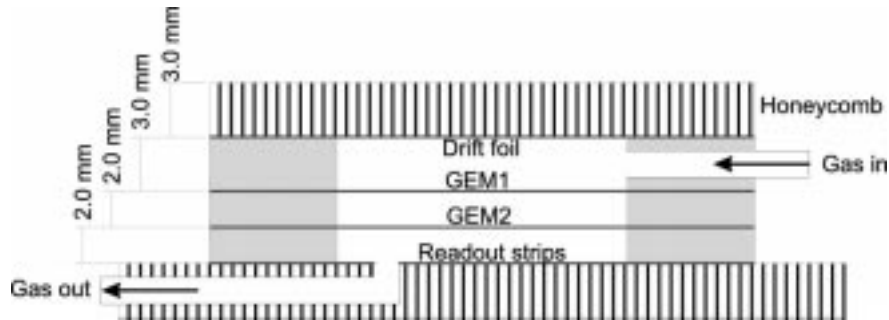


Fig. 2. Schematic cross section of a double GEM detector.

detector is operated in a gas mixture of 70% Argon and 30%  $\text{CO}_2$ . To decrease the energy stored in each foil, they are divided on one side into individually powered longitudinal sectors. The central part, a separate circular sector of 50 mm diameter, can be deactivated to allow operation in the high-intensity beams. A two-dimensional projective readout of the signal is accomplished by two orthogonal sets of parallel metal strips, engraved on the two sides of a thin Kapton foil. After gluing the foil onto a thin insulating support, the Kapton in the interstices between the strips on the upper side is chemically removed, thus opening the bottom layer of strips to charge collection. With each layer consisting of 768 strips with a pitch of  $400\ \mu\text{m}$ , the total active area per detector is  $31 \times 31\ \text{cm}^2$ . To minimize the frame material, these active components are sandwiched between two 3-mm-thick honeycomb plates with  $125\text{-}\mu\text{m}$  layers of Vetronite on either side. The larger one of these plates also serves as a support for the readout electronics and the high-voltage distribution chain. Fig. 3 shows a top view of the detector.

For the readout, we chose the APV25, an analog pipeline application-specific integrated circuit (ASIC) fabricated in  $0.25\text{-}\mu\text{m}$  CMOS technology and developed for the CMS silicon microstrip tracker [5]. The chip consists of a preamplifier and shaper stage (50 ns peaking time) for each of the 128 input channels, which are continuously sampled at 40 MHz and written into 192 memory cells. Upon receiving a trigger, the respective columns in the memory are transferred into a FIFO, allowing for a maximum trigger latency of  $4\ \mu\text{s}$ , before they are multiplexed to the analog-to-digital converter (ADC).

### III. RESULTS OF LABORATORY TESTS

The basic properties of the first COMPASS prototypes were studied extensively both in the laboratory and in various test

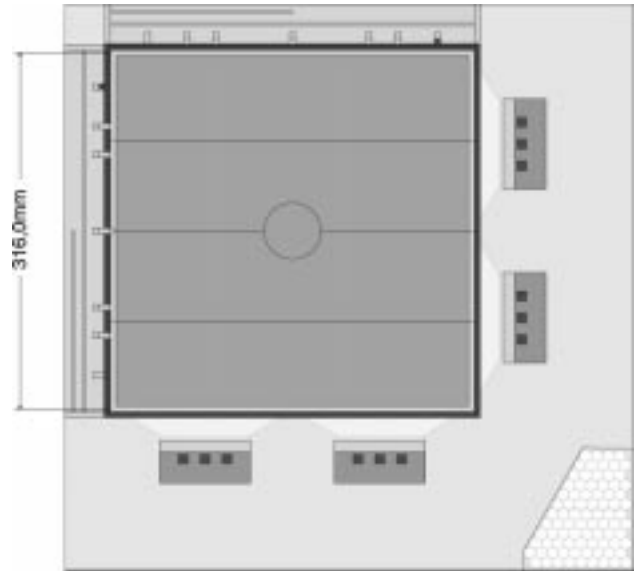


Fig. 3. Top view of a GEM detector for COMPASS.

beams at CERN and at PSI [6]. In the laboratory, we used Cu X-rays to study the energy resolution, the charge sharing between the two coordinates, and the uniformity of gain over the surface of the detector. Fig. 4 shows a pulse-height spectrum of 8.9-keV Cu X-rays for the upper and lower strip layer of the two-dimensional readout board. An almost equal charge sharing between the two coordinates was achieved by adjusting the strip widths of the upper and lower layer to 80 and  $350\ \mu\text{m}$ , respectively. The energy resolution was measured to be  $\Delta E/E \approx 22\%$ .

Since the production of the gas detector version of the APV chip (APV-M) was stopped by CMS in November 1999, and the APV25 was available only in May 2000, first noise and

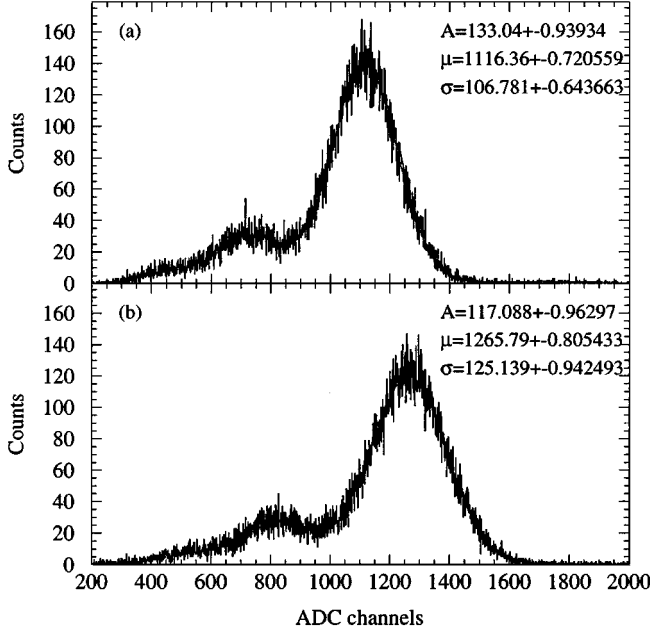


Fig. 4. Pulse-height spectrum of 8.9-keV Cu X-rays for the (a) upper and (b) lower strip layer of the two-dimensional readout board.

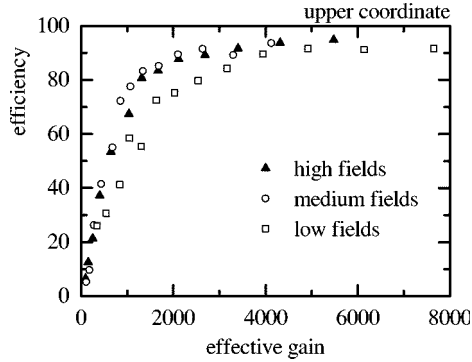


Fig. 5. Efficiency curves as a function of the effective gain per coordinate for different values of the electric fields between the two GEM foils and between the second GEM and the readout circuit, respectively. See Table I for electric field configurations.

efficiency studies of the detectors were performed using the PreMux128 chip, a predecessor of the APV chip series. Fig. 5 shows efficiency curves for different electric fields between the two GEM foils and between the second GEM and the readout circuit, respectively. At normal working conditions (“medium fields”; see Table I for field configurations), the efficiency plateau of the detector equipped with the PreMux128 was found to start at a total effective gain of 6000. (Note that the abscissa of Fig. 5 corresponds to the effective gain *per coordinate*, which is a factor of two smaller than the total effective gain.) The effective gain corresponds to the charge collected by the readout electrode and is measured by recording the signal current on each readout plane as a function of the counting rate under irradiation with 8.9-keV X-rays. Since the efficiency was measured in the laboratory with respect to a scintillator using a  $^{90}\text{Sr}$   $\beta$ -source, its absolute value is underestimated. From beam measurements with a similar detector configuration using a silicon microstrip telescope as a reference, the efficiency plateau was found to start at absolute values of  $>98\%$ .

TABLE I  
ELECTRIC FIELD CONFIGURATIONS USED DURING THE LABORATORY MEASUREMENTS.  $E_{\text{drift}}$  DENOTES THE FIELD BETWEEN THE DRIFT ELECTRODE AND THE FIRST GEM FOIL (“DRIFT FIELD”),  $E_{\text{trans}}$  THE FIELD BETWEEN THE CASCADDED GEM FOILS (“TRANSFER FIELD”), AND  $E_{\text{ind}}$  THE FIELD BETWEEN THE LAST GEM FOIL AND THE READOUT PLANE (“INDUCTION FIELD”)

		low fields	medium fields	high fields
$E_{\text{drift}}$	(kV/cm)	3.0	3.0	3.0
$E_{\text{trans}}$	(kV/cm)	2.0	4.0	4.0
$E_{\text{ind}}$	(kV/cm)	4.0	4.0	7.0

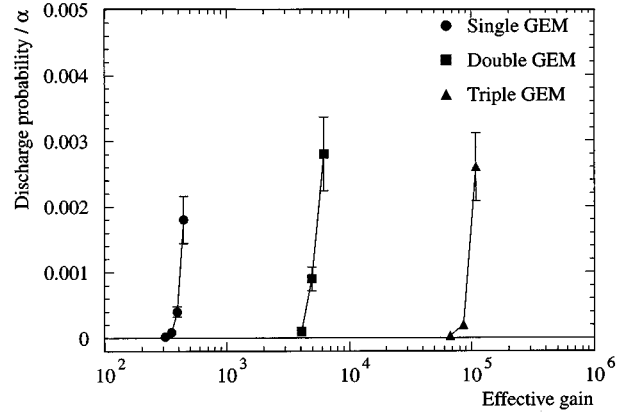


Fig. 6. Probability of a discharge, normalized to the number of  $\alpha$  decays, versus gain for single, double, and triple GEM detectors.

#### IV. DISCHARGE STUDIES

A common problem of all micropattern gas detectors is the fact that gas discharges start to occur at gains above several thousand upon exposure to heavily ionizing tracks [7]. To better understand the underlying processes and possibly find means to optimize GEM detectors so that they can operate under the hostile conditions expected in the COMPASS spectrometer, we performed systematic studies of discharges provoked by  $\alpha$  particles introduced into small  $10 \times 10 \text{ cm}^2$  GEM detectors.

Fig. 6 shows the probability that a discharge will occur, normalized to the total number of  $\alpha$  decays observed in the detector, as a function of the effective gain for a single GEM amplification stage, as well as for two and even three cascaded stages. Considering that a gain of  $\sim 6000$  is necessary in order for the COMPASS GEM detectors to be fully efficient on both readout planes, the probability of having a discharge in a double GEM structure is already sizable. Adding an additional GEM foil (“triple GEM”), this probability is reduced below our measurement limit. This is because, at a given gain, each of the GEM foils can then be operated at a much safer potential difference of  $\Delta U_{\text{GEM}} \approx 380 \text{ V}$  in contrast to  $\approx 430 \text{ V}$  for a double GEM.

Although the probability of discharges’ occurring in a GEM detector can be decreased drastically by going to a triple GEM structure, we cannot completely exclude the possibility of a discharge happening at all. To study their impact on the readout electronics, it was essential to measure the charge released to the readout circuit in a discharge. In Fig. 7(a), the voltage drop on  $25 \Omega$  during discharges is displayed for different capacitances

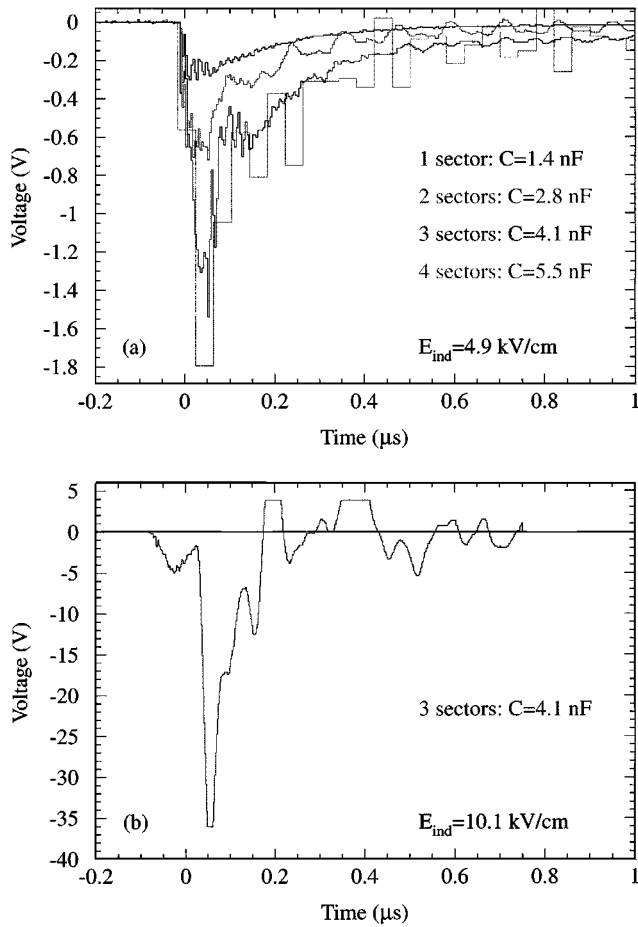


Fig. 7. Voltage drop on  $25\ \Omega$  in the case of (a) nonpropagating discharges in the GEM foil only (for different capacitances of the GEM) and (b) a discharge propagating to the readout strips.

of the second (sectorized) GEM foil (realized by connecting together individual sectors) in a double GEM device. In this case, the discharges occur between the two electrodes of the GEM foil only, the charge being released depending on the total energy stored in the foil (given by its capacitance). The fraction of the total charge collected by the readout strips depends on the electric field between the last GEM and the readout ( $\sim 2.5$ – $10$  nC at  $4.9$  kV/cm). By increasing the field strength, however, one can provoke discharges initiated in the GEM to fully propagate to the readout circuit. Fig. 7(b) shows that the voltage drop on  $25\ \Omega$  in this case may exceed  $40$  V, equivalent to instantaneous currents on the order of  $1$  A.

In Fig. 8, we show the probability of such full discharges as a function of the induction field  $E_{ind}$  between the last GEM and the readout circuit for different capacitances of GEM foils. Obviously, these full discharges can be largely avoided by staying at moderate values of  $E_{ind} = 3$ – $4$  kV/cm and, more important, by further decreasing the sector sizes. For the new COMPASS detectors, we chose a total number of 13 sectors, equivalent to a capacitance of  $\sim 5$  nF for each sector.

#### V. COMPASS BEAM IN 2000

The commissioning of the COMPASS spectrometer at the SPS of CERN started in May 2000. For this year's run, we installed a total of four large-size GEM detectors. To verify our

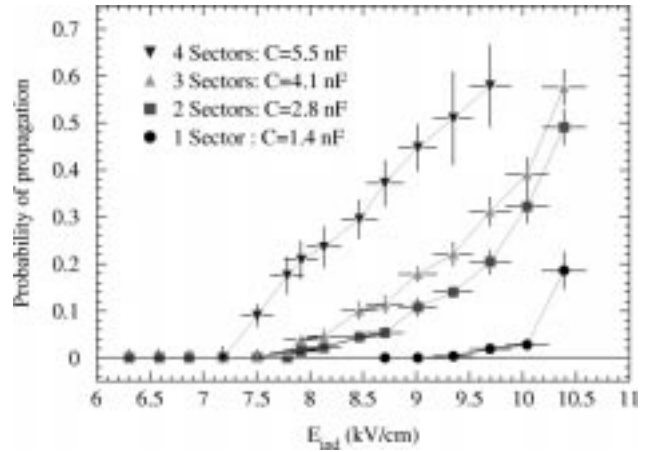


Fig. 8. Probability of full discharges to the readout strips as a function of the induction field  $E_{ind}$  between the GEM foil and the readout plane for different capacitances of the GEM foil.

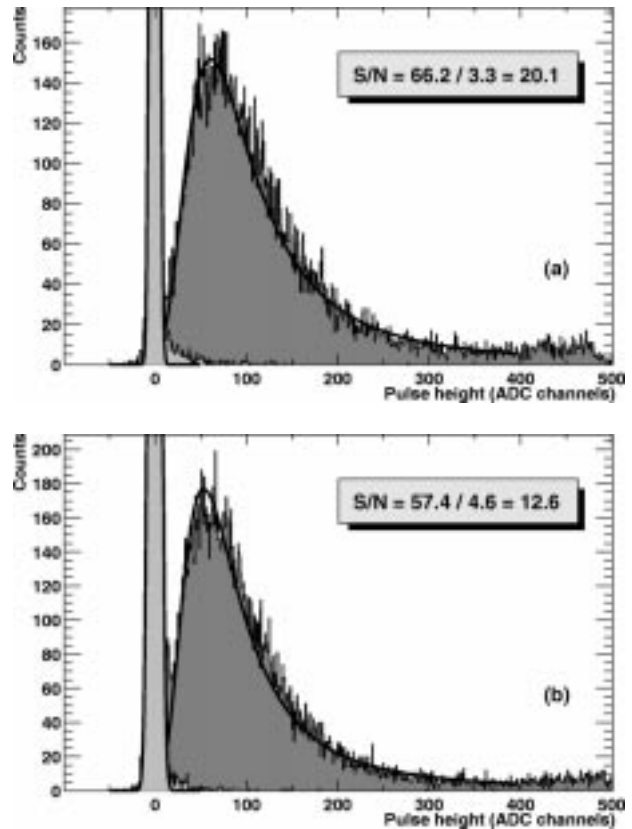


Fig. 9. Pulse-height spectra (maximum strip amplitude in ADC channels) for the (a) upper and (b) lower layer of readout strips, superimposed by the noise of an arbitrary strip. One ADC channel corresponds to  $\sim 300\ e^-$ .

laboratory results on discharges, one of them was a triple GEM detector, while the other ones only had two GEM amplification stages. Due to the late availability of the readout electronics, only one of the double GEMs was equipped with six APV25 chips, enabling us to read 384 strips on each coordinate. For first performance tests, we used a scintillator telescope to trigger on the beam halo or on interactions in the target. The central area was deactivated all the time.

Fig. 9 shows pulse-height spectra of minimum ionizing particles ( $160\ \text{GeV}\ \mu^-$ ) for the upper and lower coordinate,

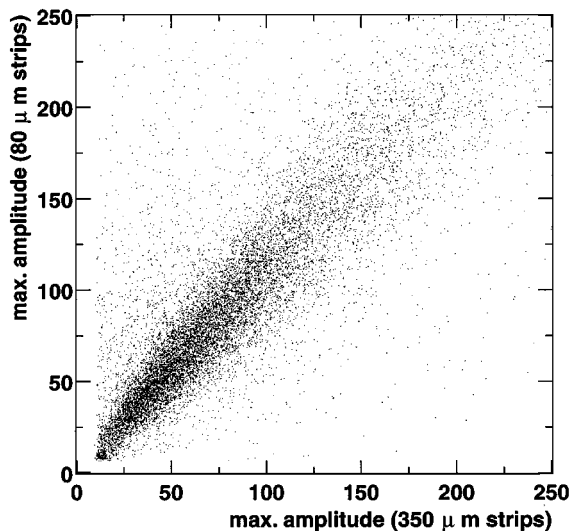


Fig. 10. Correlation of maximum strip amplitudes on the upper (width 80  $\mu\text{m}$ ) and lower (width 350  $\mu\text{m}$ ) readout layers.

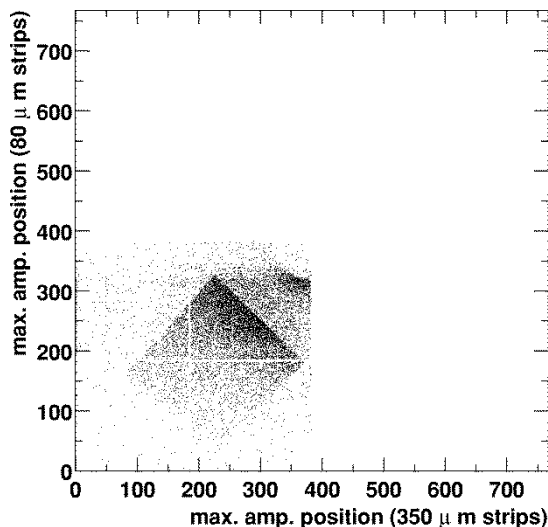


Fig. 11. Positions of strips with maximum amplitude (hit map). Only one quarter of the detector was equipped with readout electronics on both coordinates. The shadow of the scintillator telescope used for triggering, as well as the deactivated central area, are visible. The cross without hits is caused by a grid placed between GEM foils, which serves as a spacer.

respectively. Here, for each event, the maximum strip amplitude on each coordinate is plotted and no cuts are applied. The noise of an arbitrary channel is superimposed on both panels. Considering that one ADC channel corresponds to a charge of about  $300e^-$ , the noise level is  $\sim 1000e^-$  for the upper layer and  $\sim 1300e^-$  for the lower layer of strips, reflecting a slightly higher capacitance on the lower coordinate due to the smaller interstrip spacing. A clear separation between noise and the peak of the Landau distribution is visible already at  $\Delta U_{\text{GEM}} = 415\text{ V}$ , corresponding to a total effective gain of  $\sim 3000$ . The signal-to-noise ratio deduced from the single-strip pulse-height spectra shown in Fig. 9 is  $\sim 20$  for the upper coordinate and  $\sim 13$  for the lower coordinate. These two values will approach each other in a more precise analysis, which has to take into account the full charge in a cluster, known to be wider on the lower readout plane. The clear pulse-height

correlation observed between the upper and lower planes of readout strips, as displayed in Fig. 10, will be exploited to resolve ambiguities in double hits.

Fig. 11 shows a hit map produced by plotting the positions of the strips with the maximum amplitude for each event. The shadow of the scintillator placed behind the active quarter of the detector is clearly visible. The deactivation of the central region works efficiently (the detector was placed slightly higher than the center of the beam). The hits outside the scintillator are due to double hits in the high-intensity  $\mu$ -beam.

## VI. CONCLUSIONS AND OUTLOOK

Four GEM detectors were successfully operated in the COMPASS beam in 2000. One of them was for the first time read out by two orthogonal readout planes (768 channels) with the final front-end chip APV25, showing a good signal-to-noise ratio already at moderate voltages across the GEM foils. The noise performance of the detector was considerably better than observed with a previous version of the chip. Despite some tens of discharges in the detector, no electronic channels were lost.

Comparing the discharge behavior of a double and a triple GEM detector, we were able to confirm the results obtained in the laboratory: adding an additional amplification stage drastically reduces the probability of a discharge occurring on exposure to heavily ionizing particles. At the same time, the probability that a discharge initiated in the GEM foil propagates to the readout strips can be significantly decreased by further sectorization of the GEM foil. The design of the first batch of 20 GEM detectors to be built until July 2001 was modified accordingly.

## ACKNOWLEDGMENT

The GEM manufacturing technology was developed by A. Gandi and R. de Oliveira (CERN-EST-SM). The mechanical assembly of the GEM detectors was done by M. van Stenis (CERN-EP-TA1). The authors warmly acknowledge their essential contribution to the realization of this work.

## REFERENCES

- [1] The COMPASS Collaboration, "COMPASS: A proposal for a common muon and proton apparatus for structure and spectroscopy," CERN/SPSLC 96-14, SPSC/P 297, Mar. 1996.
- [2] Y. Giomataris, P. Rebougeard, J. P. Robert, and G. Charpak, "MICROMEGAS: A high-granularity position-sensitive gaseous detector for high particle-flux experiments," *Nucl. Instrum. Meth.*, vol. A376, pp. 29–35, 1996.
- [3] F. Sauli, "GEM: A new concept for electron amplification in gas detectors," *Nucl. Instrum. Meth.*, vol. A386, pp. 531–534, 1997.
- [4] F. Sauli and A. Sharma, "Micropattern gaseous detectors," *Annu. Rev. Nucl. Part. Sci.*, vol. 49, pp. 341–388, 1999.
- [5] L. L. Jones, M. J. French, Q. Morrissey, A. Neviani, M. Raymond, G. Hall, P. Moreira, and G. Cervelli, "The APV25 deep submicron readout chip for CMS detectors," in *Proc. 5th Conf. Electronics for LHC Experiments*, 1999, CERN-99-09, pp. 162–166.
- [6] S. Bachmann, A. Bressan, B. Ketzer, M. Deutel, L. Ropelewski, F. Sauli, A. Bondar, A. Buzulutskov, L. Shekhtman, A. Sokolov, A. Tatarinov, A. Vasil'ev, S. Kappler, and E. Schulte, "Performance of GEM detectors in high intensity particle beams," *Nucl. Instrum. Meth. A*, 2001. CERN-EP/2000-116, to be published.
- [7] A. Bressan, M. Hoch, P. Pagano, L. Ropelewski, F. Sauli, S. Biagi, A. Buzulutskov, M. Gruwé, G. de Lentdecker, D. Moermann, and A. Sharma, "High rate behavior and discharge limits in micro-pattern detectors," *Nucl. Instrum. Meth.*, vol. A424, pp. 321–342, 1999.